Accelerators and Beam Physics

Improvement of RF-KO System in UVSOR

A. Mochihashi, K. Hayashi, M. Hosaka, M. Katoh, J. Yamazaki, Y. Takashima*, Y. Hori**

UVSOR Facility, Institute for Molecular Science, Myodaiji, Okazaki 444-8585, Japan
**Institute for Molecular Science, Myodaiji, Okazaki 444-8585, Japan*
***High Energy Accelerator Research Organization (KEK), Tsukuba 305-0801, Japan*

In the UVSOR, a transverse stripline kicker for RF knock-out (RF-KO) has been installed in a long straight section, and the kicker has been routinely used for making empty RF-buckets in the multibunch operation to avoid multibunch instability such as ion instability[1, 2, 3]. From April to June 2002, we have improved the RF-KO system not only to reinforce the power of the RF-KO but also to rebuild a transverse tune measurement system. Moreover, the new RF-KO system can be used for a bunch-by-bunch beam handling with a high speed gated RF-KO. With the system, not only dumping particular bunches circulating in the ring but also measuring the horizontal and vertical tune have become much easier than before, and moreover, precise bunch-by-bunch beam handling, such as purification at the singlebunch operation in which spurious bunches are dumped continuously by the RF-KO without disturbing the main bunch, also becomes possible. High purity operation with the purification system in the singlebunch mode has been successfully applied since July 2002, and good purity has been kept without decreasing the beam lifetime.

In the former RF-KO system, the low level RF-KO signal from the signal generator (S.G.) and the pulse signal synchronized with revolution of the electron beam from a pulse generator called bucket-dumper were multiplied by a double balanced mixer (DBM). The pulse-modulated RF-KO signals amplified by the high power amplifier were forcibly divided and applied to each stripline because the former RF-KO system had only one high power amplifier. The power divider that divided the high level signal limited the maximum power of the RF-KO, therefore, the RF-KO power was not sufficient to dump the electron beam easily although the high power amplifier itself has good specification (maximum output power of 250 W). Moreover, it was not so easy to measure horizontal/vertical tunes with the RF-KO system because the direction of the transverse kick by the RF-KO were fixed and not able to be changed easily. To clear these problems, we have improved the RF-KO system. Figure 1 shows a block diagram of the new RF-KO system. We have prepared 4 high power amplifiers (R&K, A220-100R) that cover wide frequency range (10 kHz - 220 MHz) and have maximum power of 100 W. We have also developed a phase-switching controller that can easily change the direction of the transverse kick by the RF-KO. With these systems, not only dumping the electron beam but also measuring the horizontal/vertical tunes have become very easy.

Because the new amplifiers have good response for the pulse signal, it is possible to perform pulse-modulated RF-KO that can perturb motion of the particular bunch circulating in the ring. As a pulse generator in the low level system we have used a high speed pulse generator (Agilent Technologies, 81110A) that has short riseup/falldown time enough to single out and kick one particular bunch without disturbing adjacent bunches. As application of the RF-KO system to the users runs, we have tried to perform purification at the singlebunch operation in which spurious bunches are dumped continuously by the RF-KO without disturbing the main bunch[4]. In the former singlebunch operation, a horizontal beam scraper was used for keeping the purity by stopping the electrons that dropped out from the main bunch and captured in the next RF buckets[5]. However, with the former method, it was very difficult to keep good purity for a long time, and moreover, the beam lifetime became shorter because the horizontal scraper was inserted near the beam orbit. On the other hand, it is expected that the purification method with the gated RF-KO can keep good purity and avoid the influence on the main bunch. Figure 2 shows the output signal from the stripline in the singlebunch condition when the purification system is in operation. The signal behind the bunch signal in the figure corresponds to the gated RF-KO signal. In the purification, the frequency of the RF-KO signal has been tuned to vertical betatron frequency (2.56 MHz) and performed frequency-modulation whose modulation range is $\pm$250 kHz. To dump unnecessary bunches unexpectedly injected in front of the main bunch, the timing of the gate is firstly adjusted in front of the main bunch. After the bunches in front of the main bunch are dumped, the timing of the gate is adjusted just behind the main bunch and fixed. Figure 3 and 4 show timing spectra of the stored beam in the singlebunch condition when the horizontal scraper was used and the gated RF-KO was operated, respectively. In the observation, we injected and stored the singlebunch whose beam current is 94 mA in Fig. 3 and 71 mA in Fig. 4, and after the beam current was decreased up to about 25 mA the timing spectra was observed with a photon counting method. As seen in these figures, the spurious bunches are clearly observed when the horizontal scraper was used, however, no spurious bunches can be seen when the gated RF-KO was operated although the background counts are not small enough to observe precisely the unnecessary bunches. From these figures, the purity of the singlebunch is estimated to be $(5.4 \pm 6.3) \times 10^{-4}$ in the former purification method and $(1.9 \pm 5.0) \times 10^{-4}$ in the gated RF-KO. The purity is greatly improved, however, now it becomes difficult to measure the purity precisely because of the background count of the photon counting system. Upgrade

of the beam diagnostic system, such as the photon counting system, is one of the next subjects.

After some machine studies we have developed a high-purity and long-lifetime mode in the singlebunch condition. Figure 5 shows change in the beam lifetime on the beam current for several singlebunch operations. The beam lifetime with the gated RF-KO becomes larger than in the former purification system because the horizontal scraper inserted near the beam orbit is not necessary in the new system. We also found that using the skew quadrupole magnets are effective for increasing the beam lifetime without any influence on the users. With the gated RF-KO system and the skew quadrupole magnets, the beam lifetime has increased about 2.5 times larger than that in the former singlebunch operation. The high-purity and long-lifetime mode in the singlebunch condition has been successfully applied to the users runs since July 2002, and no troubles have been reported so far.

The authors express their sincere thanks to Dr. Obina in the High Energy Accelerator Research Organization (KEK) for his useful suggestions.

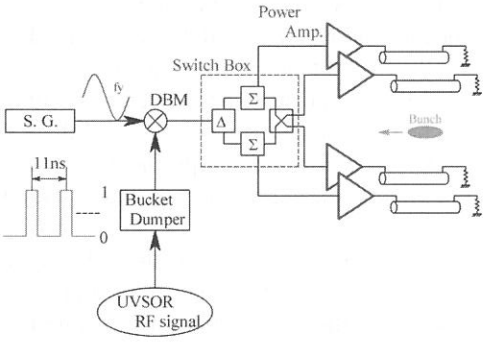

Figure 1: The block diagram of the new RF-KO system.

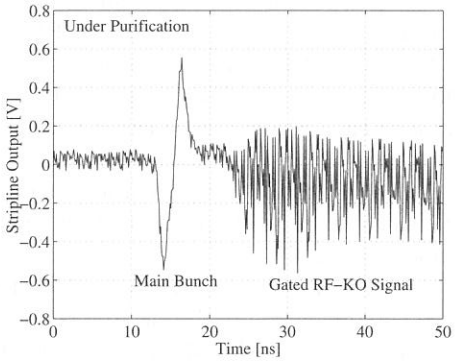

Figure 2: The output signal from the stripline in the singlebunch condition when the gated RF-KO is in operation.

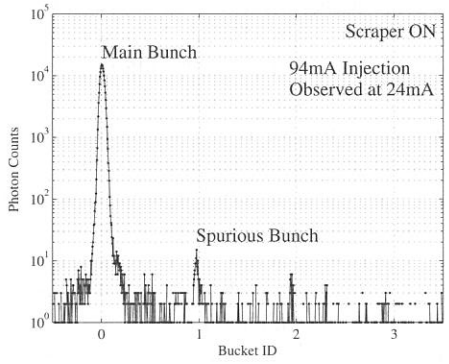

Figure 3: The timing spectrum in the singlebunch condition with the horizontal scraper.

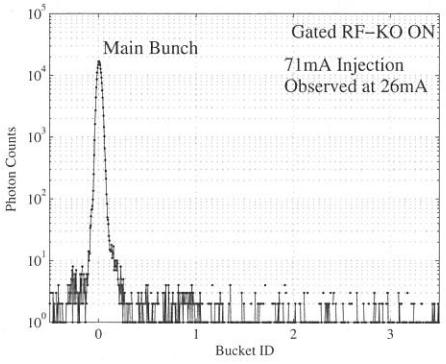

Figure 4: The timing spectrum in the singlebunch condition with the gated RF-KO.

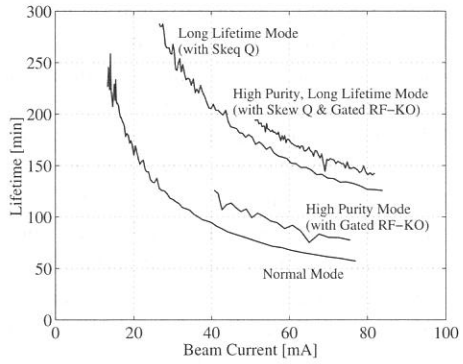

Figure 5: Change in the beam lifetime on the beam current in several singlebunch operations.

References

[1] R. D. Kohaupt, DESY Interner Bericht No. H1-71/2, 1971 (unpublished).

[2] Y. Baconnier, G. Brianti, CERN Internal Report No. CERN/SPS/80-2 (DI), 1980 (unpublished).

[3] E. Keil, B. Zotter, CERN-ISR-TH/71-58 (unpublished).

[4] T. Obina, K. Haga, T. Honda and S. Sakanaka, in *Proceedings of the 1999 Particle Accelerator Conference, New York, 1999*, edited by A. Luccio, W. MacKay, p. 2310.

[5] T. Obina *et al.*, Nucl. Instrum. Methods A **354**, 204 (1995).

Optical Beam Position Monitor in UVSOR

A. Mochihashi, K. Hayashi, M. Hosaka, M. Katoh, J. Yamazaki, E. Nakamura, Y. Takashima*, Y. Hori**

UVSOR Facility, Institute for Molecular Science, Myodaiji, Okazaki 444-8585, Japan
**Institute for Molecular Science, Myodaiji, Okazaki 444-8585, Japan*
***High Energy Accelerator Research Organization (KEK), Tsukuba 305-0801, Japan*

In the UVSOR, transverse positions of the electron beam circulating in the ring has been mainly observed with button-type beam position monitors (BPMs) that are set on the beam ducts in bending magnets (bending ducts). Because the BPMs are fixed on the bending ducts, it is difficult to observe precise beam positions because an effect of deformation of the ducts could not be negligible for the observation. To clear the problem, we have developed an optical beam position monitor that can observe the beam position by detecting a transverse position of the synchrotron radiation (SR) emitted by the electron beam. Such beam monitors have never been installed in the UVSOR before; therefore, it is the first model of the optical monitor in the UVSOR. Because the monitor is set in an SR outlet chamber that is fixed independently of the bending ducts, it is expected that the monitor can observe precisely the beam position without influence of the deformation of the beam ducts.

We have decided that the monitor is set in the SR outlet chamber in the BL-7B and designed the monitor that matches environmental condition in the beamline; namely, it is necessary to set the monitor without any influence on the SR users in the beamline. Figure 1 and 2 show a drawing and a photograph of the optical beam position monitor in the UVSOR BL-7B. Basically, the monitor has the same structure as that has used in KEK-PF[1]; namely, the monitor has a pair of triangular plates that are vertically aligned together. The plates are irradiated by the SR from the bending section, and photocurrents are induced on each plate. By measuring asymmetry of the photocurrents induced on the plates the vertical position of the SR can be detected. Because there is not much room in the outlet chamber, we have simplified the cooling system of the monitor; the plates are indirectly water-cooled by cooling a copper-mount on which the plates are set. To adjust the position of the plates to the SR axis, moving gears are settled not only for the vertical direction but also for the horizontal direction. To cope with photoelectrons that exist in the environment, a setup that can apply negative voltage (~ -50V) to the plates has been applied. The monitor was installed in the UVSOR BL-7B at August 2002 and some performance tests were carried out. Figure 3 shows measured SR position when the position of the plates are scanned vertically by a stepping motor. As seen in the figure, it is expected that the monitor has good linearity for vertical movement of the SR position. Figure 4 shows change in the measured SR position when the vertical stepping motor moves in one step that corresponds to 4 μm. From the figure, it is found that the resolution of the monitor for the vertical movement of the SR beam is less than 4 μm, that is almost the same resolution of the BPMs.

After some performance tests, we found that the optical monitor has good performance enough to measure subtle movement of the beam orbit in the routine operation in real time. Figure 5 shows an example of a measured vertical position of the SR for one day. As seen in the figure, the monitor can see a drift of the SR position in the vertical direction for one day although the monitor tends to be affected by the operation of the beam shutter because the shutter is settled near the monitor. The measured position seems to drift in several 10 μ m for one day; the tendency roughly corresponds to the measurement with the BPM system. From Fig. 4 and 5 it is expected that the monitor can be used not only for the usual beam diagnosis in the routine users runs but also for check distortion of the beam orbit due to free-tuning of the in-vacuum undulators that have been installed in the BL-7U and BL-3U[2, 3] in the UVSOR-II. Now we are developing a control system and a data acquisition system for the optical monitor. After the development we are planning to apply the monitor to one of the beam diagnostic tools for the routine operation in the UVSOR-II.

The authors express their sincere thanks to Dr. Mitsuhashi and Mr. Tadano in the High Energy Accelerator Research Organization (KEK) for their useful suggestions.

References

[1] Photon Factory Activity Report 2000, p. 87.

[2] M. Katoh *et al.*,
UVSOR Activity Report 2000, p. 37.

[3] A. Mochihashi *et al.*,
UVSOR Activity Report 2001, p. 47.

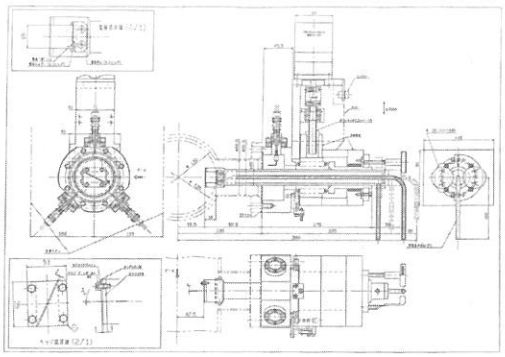

Figure 1: Drawing of the optical beam position monitor in the UVSOR BL-7B.

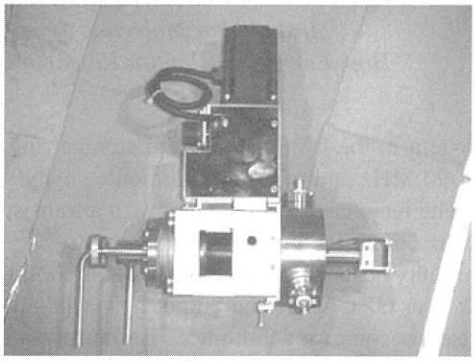

Figure 2: Photograph of the optical beam position monitor.

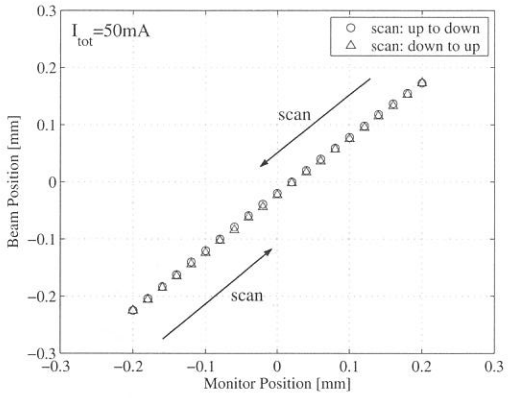

Figure 3: Change in the measured vertical SR position when the monitor is scanned vertically in $\pm 200 \mu$m.

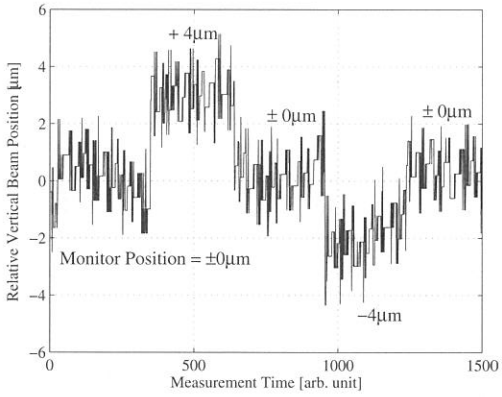

Figure 4: Change in the measured vertical SR position when the monitor moves in one step (4μm) of the stepping motor.

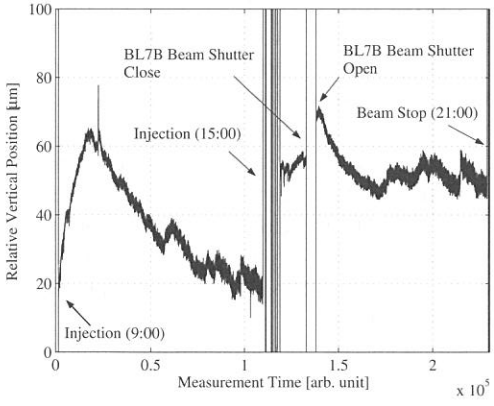

Figure 5: An example of the vertical SR position measured with the optical beam position monitor for one day.

New RF Coupler for Main Cavity in UVSOR

A. Mochihashi, K. Hayashi, M. Hosaka, M. Katoh, J. Yamazaki, Y. Takashima*, Y. Hori**

UVSOR Facility, Institute for Molecular Science, Myodaiji, Okazaki 444-8585, Japan
**Institute for Molecular Science, Myodaiji, Okazaki 444-8585, Japan*
***High Energy Accelerator Research Organization (KEK), Tsukuba 305-0801, Japan*

An RF-system in the UVSOR electron storage ring is composed both of a main RF-cavity whose resonant frequency of 90 MHz and of a third harmonic cavity. Table 1 show the main parameters of the main cavity in the UVSOR. The main cavity is operated with a transistor-type transmitter whose maximum output power is 20 kW, however, the output RF power is limited up to 7 kW in routine multibunch operation because an input RF coupler abnormally heats up. Even though an air cooling system is operated, the temperature of waveguides near the coupler is over 60°C when the output power is only 6 kW; therefore, it is supposed that the temperature of the coupler itself becomes much higher. To improve a beam lifetime larger and to compress bunch length shorter it is strongly desired to increase an RF voltage V_c (V_c = 46 kV in the routine operation) by increasing the output RF power; however, it is very difficult to increase the power because of the heating problem. In the past, we have an experience that when the main cavity was in operation a ceramic window of the RF coupler cracked and the vacuum condition in the cavity was troubled. From the experience, it is supposed that not only the inner and outer conductors of the coupler but also the ceramic window get heat; however, the RF loss at the ceramic window is estimated to be very small. We have considered that it is the cause of the heating that not only the RF loss but also a multipact phenomenon that locally occurs between the inner and outer conductors through the surface of the ceramic window.

From the point of view, we have designed a new RF coupler that can cope with the multipact phenomenon. Basically, the new coupler has the same configuration as the old one, however, it has some improved points; to suppress the RF loss in the coupling loop the thickness of the loop has been improved (from 1 mm to 3 mm). Another point is that to suppress emission of secondary electrons that cause the multipact phenomenon TiN has been coated (coating thickness is 100 Å) on the surface of the ceramic window. Figure 1 and 2 show the photographs of the new RF coupler. The size of the coupler is 120 mm in diameter and 220 mm in length without the coupling loop. The inner and outer conductors are made of oxygen-free copper, and the joint between the coupler and the waveguides are made of oxygen-free copper coated with gold. The coupler was installed in the main cavity at April 2002 and some performance tests were carried out. As a result, the dangerous heating has been completely suppressed; when the output power is 7 kW the temperature of the waveguides near the coupler is reduced to about only 30°C. The coupler has been currently used in the routine operation without any trouble.

Next, we have tried to increase the RF voltage in the main cavity and observed the change in the beam lifetime. Figure 3 shows the beam current and the beam lifetime in the single/multi bunch conditions when the cavity voltage was increased to about 60 kV. When the multibunch condition whose beam current is 300 mA, the $I\tau$ value that is 1700 mA·Hour in the routine cavity voltage (V_c = 46kV) was improved to 1950 mA·Hour in V_c = 61kV that corresponds to the output power of 8 kW. On the other hand, when the singlebunch condition whose beam current is 90mA, the $I\tau$ value that is 30 mA·Hour in the routine cavity voltage and without skew-Q magnets was improved to 80 mA·Hour in V_c = 63kV without the skew-Q magnets. We have also tried to increase the cavity voltage more and more by increasing the output power, however, we found that as the power is increased it becomes difficult to store the electron beam stably because in such high power operation the cavity tends to be largely detuned and it is necessary to adjust a tuner position beyond movable reach of the tuner. To increase more the output power and realize the high power operation routinely and stably, therefore, it is necessary to improve the cooling system of the cavity itself. We are now planning not only the improvement of the current RF system but also an renewal project of the RF cavity to improve quality of the electron beam in the UVSOR-II.

The authors express their sincere thanks to Dr. Y. Saitoh, Dr. F. Naitoh and Dr. T. Kasuga in the High Energy Accelerator Research Organization (KEK) for their useful suggestions.

Table 1: Main parameters of the main cavity of the UVSOR-ring.

Frequency	90.1	MHz
Harmonic Number	16	
Q-factor	3000	(Loaded)
Shunt Impedance	500	kΩ
Cavity Voltage	46	kV (routine)
Number of Cavity	1	
Bucket Height	7.5×10^{-3}	
Maximum Output Power	20	kW

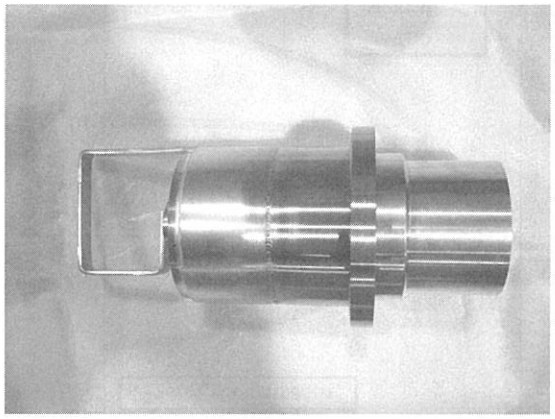

Figure 1: Photograph of the new RF coupler for the main cavity of the UVSOR-ring.

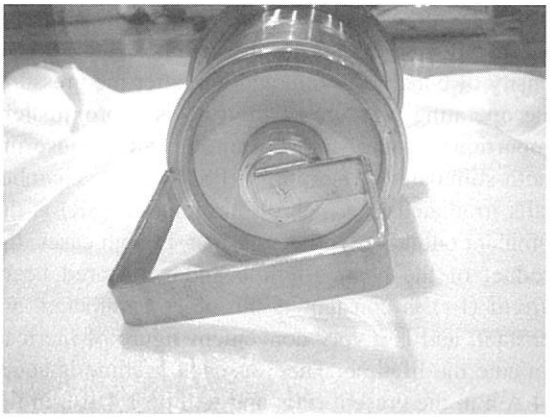

Figure 2: From the view of the ceramic window and the coupling loop.

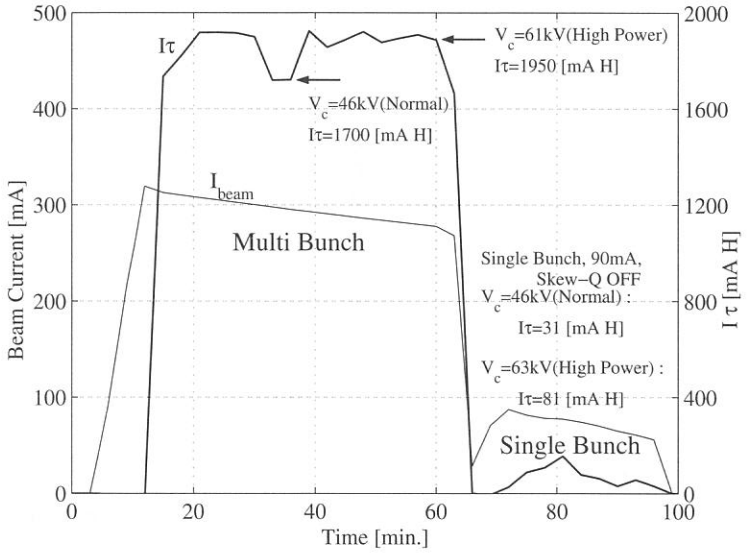

Figure 3: Beam current and Iτ value when the high power operation of the RF system. Iτ values increased by about 20% and 250% in multibunch and singlebunch conditions in the high power operation.

Vacuum consideration for the UVSOR II

Yoichiro HORI, Jun-Ichiro YAMAZAKI, Masahiro KATOH, Kenji HAYASHI,
Masahito HOSAKA and Akira MOCHIHASHI

UVSOR facility, Institute for Molecular science, Myodaiiji, Okazaki, 444-8585 Japan

In the UVSOR upgrade (UVSOR II) project, a number of vacuum beam chambers should be replaced new ones compatible to the new magnets and the improvements of beam-lines. Some vacuum problems have been discussed for designing new chambers.

1. Pressure and beam lifetime

Main processes of beam loss are the Touschek effect, that is electron-electron collision in bunch, and collision with residual gases in the UVSOR ring. The former collision occurs in proportion to the number density of bunch electron, and the latter the pressure. The operating pressure of the ring is approximately proportional to the stored beam current because the photo-stimulated desorption (PSD) from chamber walls irradiated by synchrotron radiation (SR) is the dominant outgassing process. Then, in both cases, the product of the beam lifetime and the stored beam current ($I \cdot \tau$) is constant if the other parameters are constant, and is a very convenient figure of merit to evaluate the lifetime. The Touschek lifetime is about 2.4 A·h in the present ring, and will be 1.4 A·h in the upgraded ring [1].

The vacuum lifetime also strongly depends on the physical aperture in the ring as shown in Fig. 1-a, in which the cross section of the vacuum beam loss is also shown. The lifetime is calculated at the CO equivalent normalized pressure of 1 E-6 Pa/A. The conversion factor of the measured pressure to the CO equivalent pressure is about 0.5 [2]. The horizontal axis is the half value of the minimum physical aperture. It is determined to 11 mm in present ring by a narrow beam channel at an insertion device, and will be 5 – 11 mm depending on the gap of a new insertion device after upgraded. Present lifetime observed at 200 mA storage is about 6 h. It means that the practical operating pressure is about 2 E-6 Pa/A (CO equiv.). If the pressure will be maintained, the lifetime would be 2.5 – 4.5 h in the future. It is also expected from Fig. 1-b that decreasing the pressure in 1 E-6 to 1 E-7 Pa range is effective to improve the lifetime, but further decreasing is inefficient and impractical.

The pressure distribution of the ring is determined by the outgassing rate, the pumping speed and the conductance in each place and can be simulated by a simple one-dimensional calculation. The pumping speed and its distribution are assumed like Fig. 2-a. The present distribution at 400 mA storage is simulated as shown in Fig. 2-b. The average pressure of 2.5 E-7 Pa has been obtained when the PSD yield is 1 E-6 molecules/photon as a constant

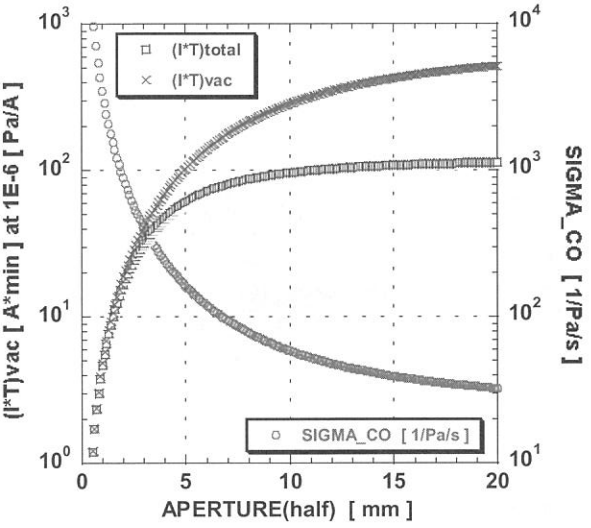

Fig.1-a Beam lifetime and vacuum beam loss constant as functions of aperture.

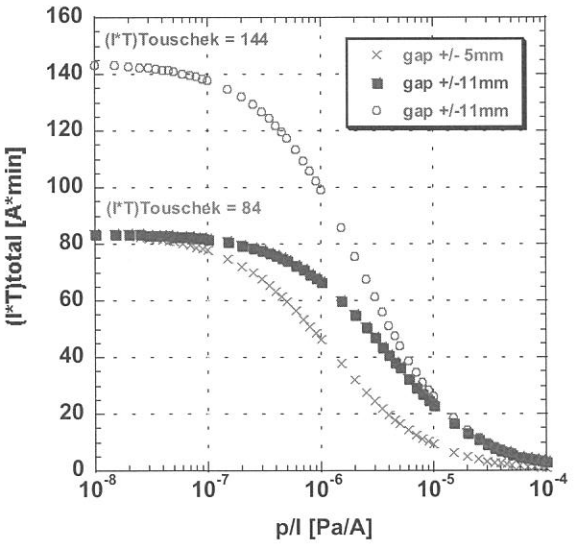

Fig.1-b Beam lifetime as a function of pressure.

value. The lifetime of 7.5 h is expected from the resulting average pressure, and it is approximate to the observed value. The distribution of outgassing rate is also given in the figure. Though there are many assumptions, it is clear the that intense irradiation with relatively small pumping speed results a high local pressure at bending sections. This suggests, however, the increasing pumping speed at these sections is effective to decrease the pressure. Same simulation expects that the lifetime can be improved by 10 - 30 % by increasing the pumping speed by factor of 2 – 4 at these sections. Further improvement is dependent on the elongation of the Touschek lifetime.

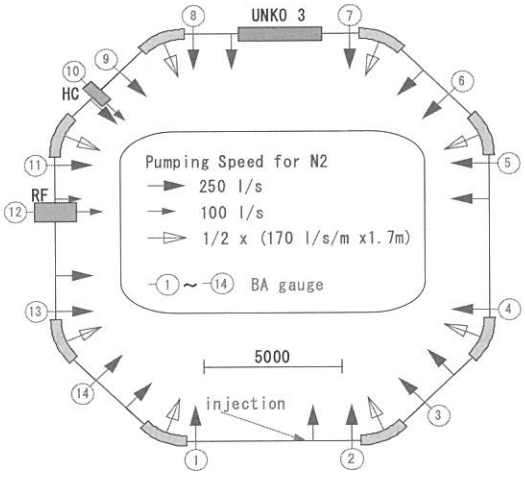

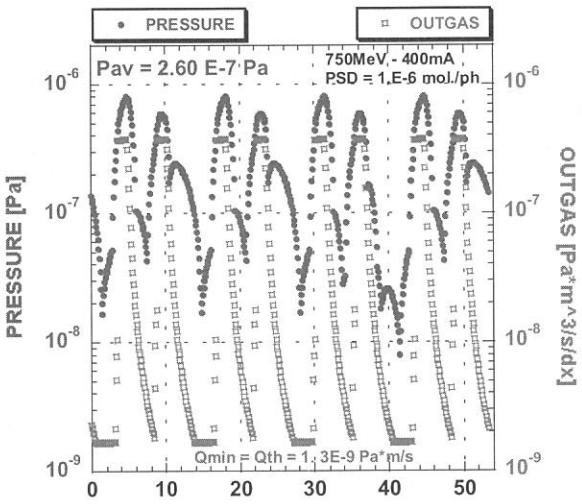

Fig.2-a Pump arrangement of the ring. Titanium sublimation pump and sputter ion pump are used.

2. Thermal/structural analysis for SR irradiation at 500 mA storage

Radiation power emitted at a bend is 1 kW/rad or 460 W/m at the maximum stored current of 500 mA. Distance between the chamber wall and the light source point is about 50 cm in the bend. Sidewall of the bend chamber suffers from up to 460 W/m of the SR load, and normally irradiated parts, such as photon absorber, suffers from up to 2.0 kW/m. It is not so serious for conventional chamber materials. Stainless steal is enough as a chamber material, and copper material is desirable for some absorbers installed near the bend.

A two-dimensional thermal/structural analysis was carried out for a stainless steel beam chamber. The analysis model is shown in Fig. 3. Cross section of the beam channel is a racetrack with the thickness of 3 mm, which is same as a present standard chamber. The heat transfer coefficient of 3000 W/m^2/K is assumed on water boundary for the water-cooling, and 10 W/m^2/K on air boundary for air-cooling. These can be very easily obtained. Results are listed in Table 1. In both case the stress is less than the yield strength, but the temperature rise is rather high in the case of air-cooling. The 0.2% strength of SuS316 is 2.05E-8 Pa. Also the deformation should be considered, especially in BPM sections. The above applies to bending section. Power load sharply reduces as the target is off from the bend, since the bending radius is small, so that air-cooling may be enough for downstream components.

Table 1 Temperature rise, stress, and deformation by SR irradiation at 500 mA storage.

	ΔTmax [deg.]	Δmax [Pa]	ΔXmax [mm]	ΔYmax [mm]
water-cooling	42	6.04E7	0.13	0.12
air-cooling	268	6.38E7	0.35	0.075

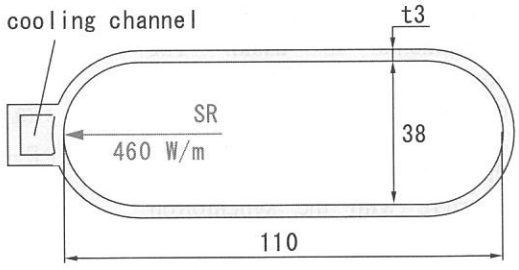

Fig.3 Shape of the analytical model.

References

[1] M.Katoh: UVSOR-LS-NOTE-001130MK.
[2] Y. Hori: *Applied Surface Science,* **169-170** (2001) 724-727.

Vacuum Chamber Design for the UVSOR II

Jun-Ichiro YAMAZAKI, Kaiichi HAGA[A] , Yoichiro HORI, Masahiro KATOH, Kenji HAYASHI, Masahito HOSAKA and Akira MOCHIHASHI

UVSOR facility, Institute for Molecular science, Myodaiiji, Okazaki, 444-8585 Japan
[A]Photon Factory, Institute of Materials Structure Science,
High Energy Accelerator Research Organization (KEK), Tsukuba, 305-0801, Japan

In the UVSOR upgrade (UVSOR II) project, all straight chambers and three bend chambers except some elements such as RF cavities and insertion devices should be replaced to new ones. Also beam position monitors (BPMs) will be newly installed at up- and down-stream in each long straight section. It is important for the effective pumping to increase the pumping speed as much as possible in the bend section and the just downstream. New chambers have been designed and fabricated, and will be installed in the UVSOR II in FY2003.

1. Straight chamber design at the quadrupole magnet

According to the new magnet arrangement [1], beam chambers installed in straight sections must be replaced to new ones. The boundary condition with existing bend chamber is not changed. Each two quadrupole magnets are installed in the up- and down-stream of every straight section. The pumping is essential between neighboring quadruple magnets, because the BPM mounted at the downstream of the bend chamber occupies an effective position for pumping. More than 200 l/s of the pumping speed is required to maintain a present efficiency. A schematic chamber design is shown in Fig. 1. It is a symmetry configuration in up- and down-stream of the straight section. Main pumps are the titanium sublimation pump (TSP) and sputter ion pump (SIP) as the present. The TSP is installed close to the beam channel in order to obtain a required pumping speed. Each two BPMs will be additionally installed in the long straight section.

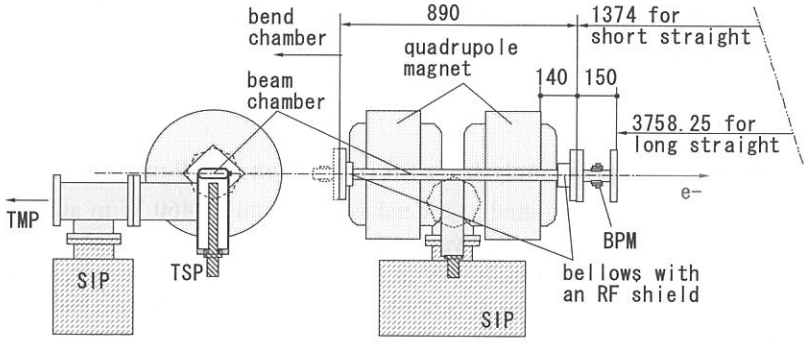

Fig.1 Straight chamber installed in quadrupole magnets

2. Bend chamber design

Three bend chambers, B3, B6 and B7, have been remodeled according to the improvement of beam-lines. Basic form is inherited from old one. The first problem is how to increase the pumping speed. In the present chamber, distributed ion pump (DIP) is already installed in the inside of the beam channel and BPMs are mounted at the up- and down-stream. The additional pumping can be inevitably installed only in the outside of the beam channel. It is most convenient and effective to install the additional pumping at junction with the beam-line if the pumping space is ensured there. But those spaces are already occupied by beam-line components in usual. The considerable second best way is equipping the pump between and/or in the upstream outside of the coil as long as it does not interfere with the synchrotron radiation light to be introduced to the beam-line. Actual design of the chambers is determined under the boundary condition with beam-lines, as shown in Figs. 2 and 3. The B7 chamber is similar to the B3. The B6 chamber has a

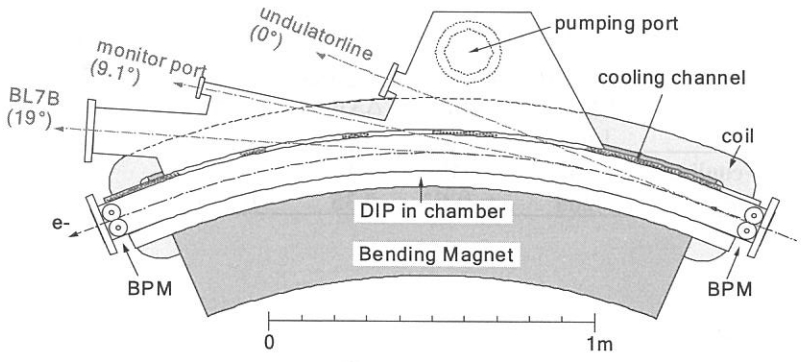

Fig. 2 Conceptual design of the bend chamber B3

special shape including an optical mirror inside. Increase of the pumping speed is considered in each chamber.

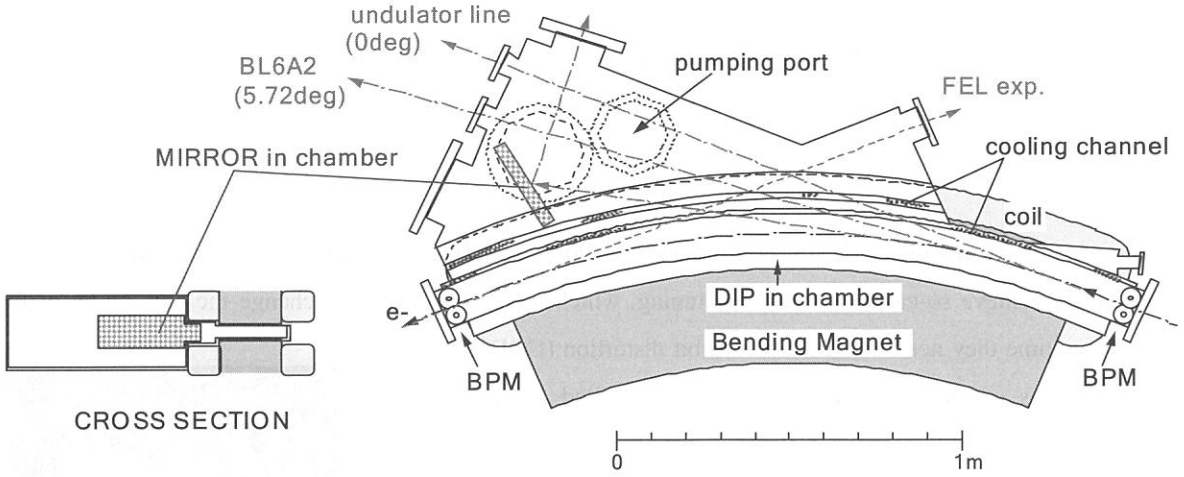

Fig. 3 Conceptual design of the bend chamber B6

3. BPM chamber design

The BPM consists of four electrodes that each two is mounted on top and bottom side of the beam channel. Sensitivities Sx and Sy of the BPM are defined as

$$x=U(x,y)/Sx,\ y=V(x,y)/Sy,$$

where x and y are position coordinates of the beam, and U(x,y) and V(x,y) are coefficients made from the charge induced in each electrode by the beam. The sensitivities depend on the electrode layout, and that of the present BPM is not proper in view of the sensitivity. The mapping simulation was carried out by a boundary element method in order to improve the vertical sensitivity Sy. The present sensitivity is 0.0792 in the horizontal and 0.0226 in the vertical. The horizontal distance between two electrodes is rather long in the present layout and it causes the low vertical sensitivity. It was found by the simulation that the vertical sensitivity could be improved in the 1.5 – 2 times without reducing the horizontal sensitivity so much by making the electrode small and shortening the horizontal distance. The decrease of the signal output can be sufficiently supplemented by electrical amplification. This concept is adopted in the BPM newly installed. Fig. 4 shows the chamber design and electrode-layout of the new BPM. The sensitivity is 0.0735 in the horizontal and 0.0376 in the vertical.

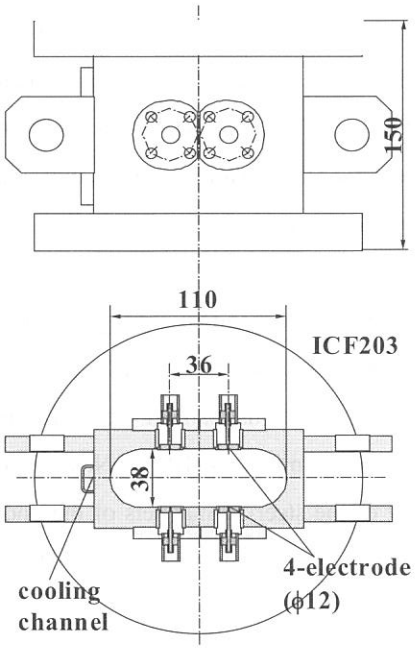

The vertical position error up to 200 μm can occur in each electrode, and it induces an offset of the electrical center of the BPM. The offset was estimated using the same simulation. The result shows vertical shift up to 190 μm and horizontal offset up to 90 μm can be introduced by each position error. These offsets should be measured and corrected by some method such as electrical mapping or beam-based calibration.

Reference

[1] M.Katoh et al., NIM in Physical Research **A467-468** (2001) 68-71.

Study on Independent Tuning of Undulator at UVSOR

K. Hayashi, M. Katoh, M. Hosaka, A. Mochihashi and J. Yamazaki

Institute for Molecular Science, Myodaiji, Okazaki 444-8585, Japan

1. Introduction

An in-vacuum type undulator (U7) was installed at UVSOR in spring 2003 (Fig. 1)[1]. A machine study was carried out to achieve so-called independent tuning, which mean that users can change the gap length of the undulator anytime they need to. The closed orbit distortion (COD) caused by gap change was corrected by steering magnets installed at upstream and downstream of the undulator magnet. Latest result of the study is reported.

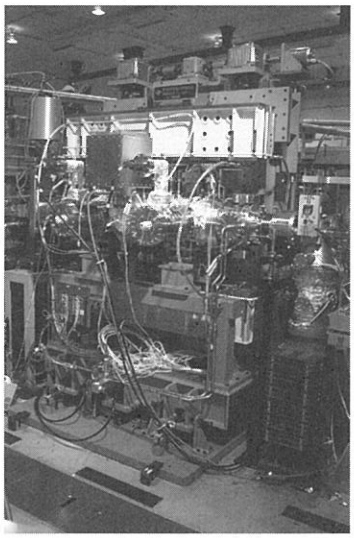

Fig.1 in-vacuum undulator (U7)

2. In-Vacuum Undulator at UVSOR

The undulator is installed at a straight section (S7) of UVSOR. It employs a control software which works on local area network, so that beamline users can change the gap length at the experimental stations. However, it was found that the gap change causes considerable COD (Fig. 2), producing a serious problem for other beamlines. Thus the COD must be eliminated to achieve the independent tuning.

3. Study on Independent Tuning of Undulator

We compensate the COD due to gap change of the undulator by using a pair of local steering magnets installed upstream and downstream of the undulator. At first, COD response to undulator gap length was measured by beam position monitors (BPM). Next, COD response to steering magnets was measured changing the excitation current of the steering magnets of the undulator. Then, with these two results the currents of the steering were determined so as to minimize the COD. We used least-square method, that is to find local minimum of S given below;

$$S = \sum_{i=1}^{N_{BPM}} \begin{Bmatrix} (x_i + u_i^H I_H)^2 \\ (y_i + v_i^V I_v)^2 \end{Bmatrix}$$

where u_i^H, I_H and x_i represent horizontal response of i-th BPM to horizontal steering magnets for unit current, excitation current of horizontal steering magnets and horizontal response of i-th BPM to gap length change, respectively. The currents of upstream horizontal and downstream horizontal magnets were set to the identical value, in the same way as upstream vertical and downstream vertical magnets. After the correction, the COD caused by gap change from 40mm to 18mm was reduced from order of 100 μ m to 10 μ m (Fig.3).

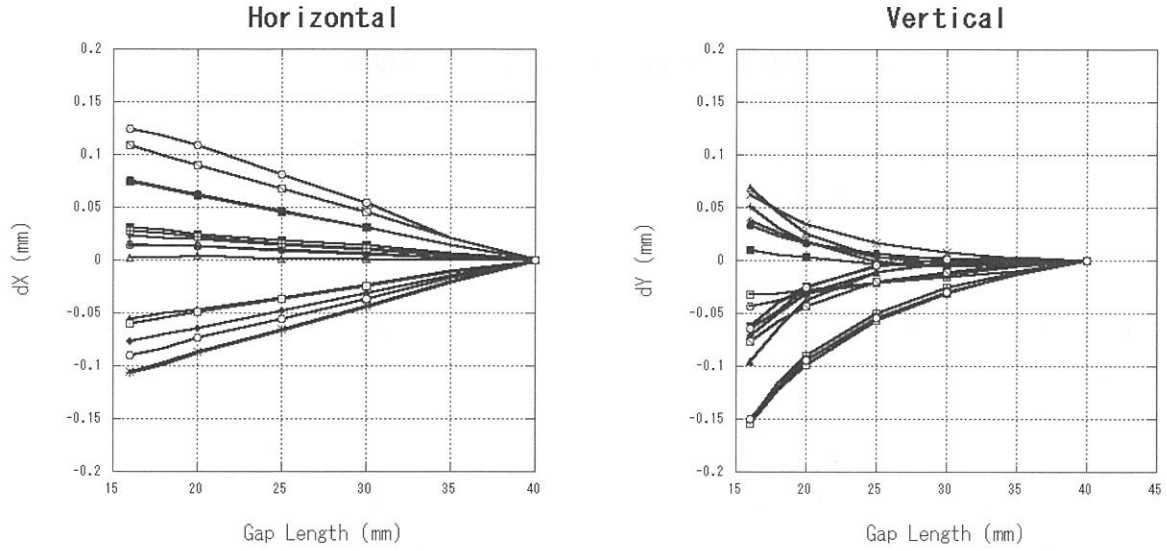

Fig. 2 COD caused by gap length change without correction (result of 16 BPMs are shown)

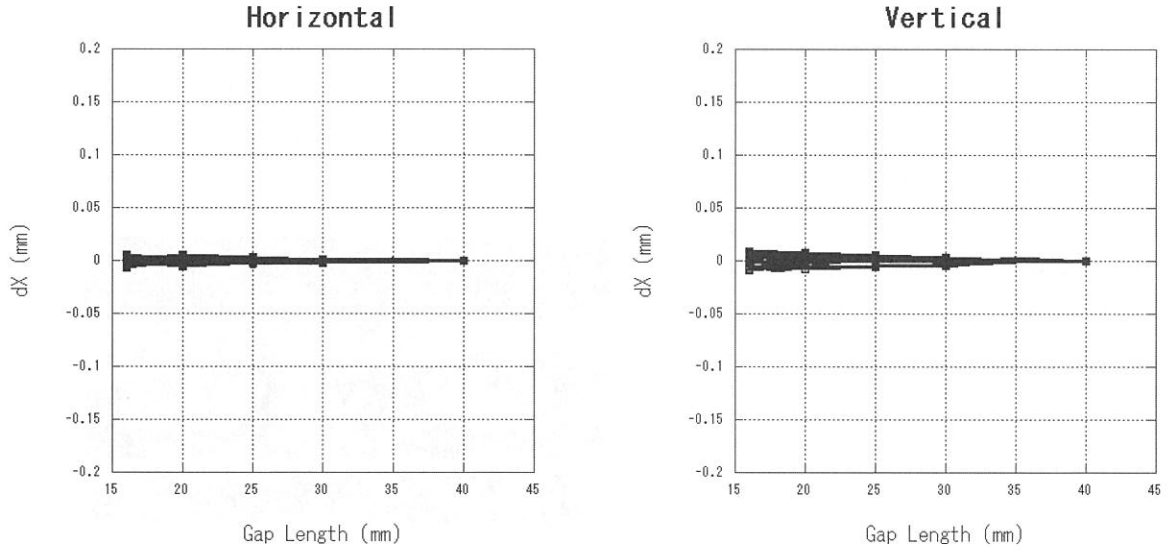

Fig. 3 COD with correction by steering magnets (result of 16 BPMs are shown)

4. Conclusion

The COD caused by gap change of the undulator was reduced to about one tenth of the case without correction. We are going to suppress the COD to smaller value utilizing extended methods, such as individual (i.e. upstream horizontal, upstream vertical, downstream horizontal, downstream vertical) optimization of steering magnet current and taking account of xy coupling. The independent tuning technique developed in our study will be soon applied to beamline 7U and same procedure will be applied to another new undulator, namely U3, which is going to be installed in spring 2003.

References

[1] A. Mochihashi et al, UVSOR Activity Report 2001, p47

Q-Switching Operation of the UVSOR-FEL

M. Hosaka, M. Katoh, A, Mochihashi, J. Yamazaki , K. Hayashi Y. Takashima and H. Hama[a]

UVSOR Facility, Institute for Molecular Science, Myodaiji, Okazaki 444 Japan

[a]Laboratory of Nuclear Science, Tohoku University, Sendai 980 Japan

The output power of a storage ring free electron laser (SRFEL) operated in the CW mode is limited by bunch heating effect due to the FEL interaction. On the other hand, much larger peak power (~100 times at the UVSOR) in a macropulse can be obtained by using Q-switching technique because lasing is started from a completely damped state of the energy spread of the electron bunch. On the UVSOR storage ring, the Q-switching operation is performed by using an rf modulation method in which the synchronism between an optical pulse and an electron bunch is detuned by varying an accelerating rf frequency fed from a master oscillator [1]. When the optical gain is small, the detuning range of the rf frequency is relatively narrow, so that the small frequency jump is sufficient to kill the lasing, and consequently the residul amplitude of excited synchrotron oscillation of the electron bunch is negligible as compared with the natural energy spread of the electron bunch. However we have recently stored a very high beam current, more than 100 mA/bunch for user application and the FEL gain at the current is estimated to be >~ 5% . Because of the higher FEL gain and the bunch lengthening, the relative detuning range of the rf frequency is getting to be more than 10^{-5} and therefore the amplitude of the synchrotron oscillation is supposed to be no longer negligible.

In order to examine the influence of the rf modulation to the longitudinal dynamics of the electron bunch, we have observed the evolution of the bunch profile by using a dual-sweep streak camera. Figure 1 shows longitudinal collective motions of the electron bunch observed when the rf frequency is suddenly changed by 2 kHz. As seen in the figure, the synchrotron oscillation is excited with relatively large amplitude. However, particularly one at the higher beam current, the measured amplitude of the synchrotron oscillation of the beam bunch is damped much faster than synchrotron radiation damping time (~ 20 ms). This fast damping can be explained as Robinson damping [2], which occurs in the interaction between the beam frequency spectrum and the cavity impedance. Thus the damping depends on a tuning angle of the rf cavity. As the tuning angle is made more negative the damping increases and if the tuning angle is positive the oscillations are anti-damped. Figure 2 shows the measured damping decrement α_R of the oscillation as a function of the tuning angle. In the measurement the tuning

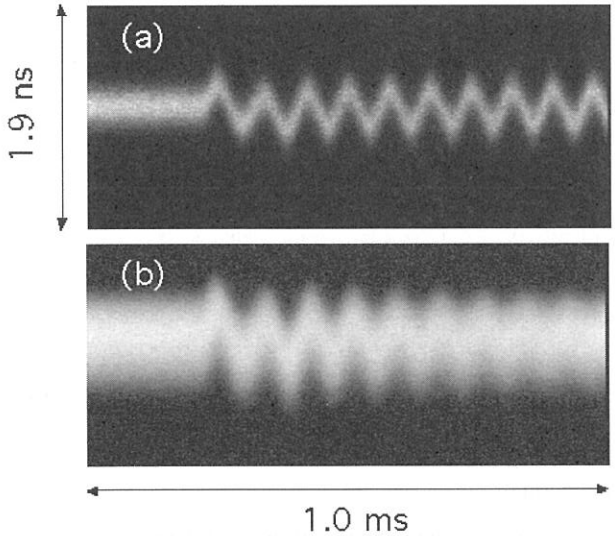

Fig. 1 Collective synchrotron oscillation excited by the rf modulation at beam current of (a) 1.0 mA and (b) 45 mA measured by a dual-sweep streak camera.

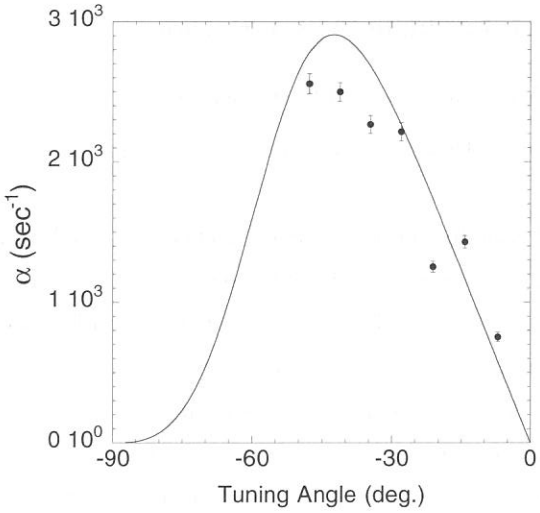

Fig. 2 Synchrotron damping decrements measured as a function of the tuning angle of the rf cavity. The solid curve is a calculated value based on Robinson damping model.

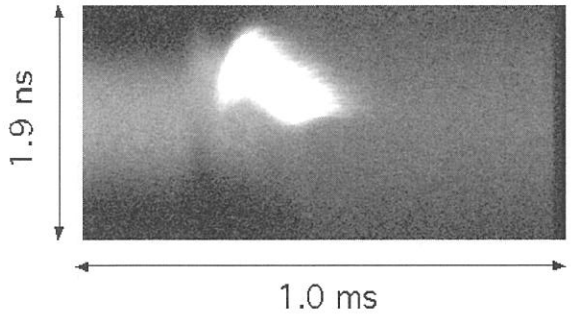

Fig. 3 Two-dimensional spectrum of the Q-switched FEL together with beam bunch. Due to the bunch heating, the bunch is very broad shortly after lasing.

angle is varied using a tuner of the rf cavity and the damping decrements are deduced from the streak camera data. An calculation based on the cavity impedance model was performed and the result is also plotted in the figure. As seen in the figure, the calculation is almost consistent with the experiment.

Besides such overall properties of the oscillation, we observed the evolution of the Q-switched FEL macropulse and the electron bunch simultaneously by using a streak camera. In order to reduce the laser intensity, which is much higher than the spontaneous radiation, a band-pass-filter of 540 nm was used for the measurement of the 570 nm lasing. Typical temporal spectrum taken with a beam current of 140 mA/2-bunch and an rf frequency jump of 1.6 kHz is shown in Fig. 3. In order to maximize Robinson damping decrement, the cavity tuning angle of 40 deg. was chosen, in which the calculated damping time is 100 μsec. As seen in the figure, the lasing gets start just after the first cycle of the collective oscillation executed by the frequency jump. It was found to be clear that Robinson damping is a crucial phenomenon for the Q-switched lasing driven by the rf modulation method.

References

[1] M. Hosaka, S. Koda, M. Katoh, J.Yamazaki, K. Hayshi, K. Takashima, T. Gejo and H. Hama, Nucl. Instr. and Meth. A 483 (2002) 146.

[2] K. W. Robinson, CEAL-1010, Feb 1964.

Challenge to High Power FEL Lasing in the UV Region

M. Hosaka, M. Katoh, A, Mochihashi, J. Yamazaki , K. Hayashi, Y. Takashima

UVSOR Facility, Institute for Molecular Science, Myodaiji, Okazaki 444-8585 Japan

An out-coupled power of a storage ring FEL is critical issue for application experiments. On the UVSOR, an out-coupled power of a storage ring FEL in the visible region (around 570 nm and 420 nm) has exceeded 0.5 W and then thus high power FEL was used for user applications. Recently there is a demand from biomolecule studies for circular polarized UV light whose helicity can be switched [1]. The UVSOR-FEL source can meet such demand because the lasing has already been achieved down to 240 nm in 1997 [2] and the helicity switch of the laser can be made freely by changing the phase of the helical undulator. However in the former experiment, the out-coupled FEL power at the wavelength was small (<1mW) as a result of low FEL gain at that time. Recently we can store the electron beam of more than 50 mA/bunch in the storage ring and expected FEL gain is around 1.7 % (Fig. 1) in the UV region. This allows to employ high efficiency mirror for the lasing and hence much increased out-coupled power in the UV region is expected.

An experiment on high power UV lasing was planned targeting wavelength of 240 nm. We have employed multi-layers of HfO_2/SiO_2 on silica substrate for the cavity mirrors since this multi-layers show good optical property, namely low absorption coefficient and high reflectivity at the wavelength. It is important to choose appropriate number of layers for high power lasing as well as mirror material. In general, an out-coupled power of a FEL is proportional to a cavity efficiency defined as (transmittance of a mirror)/(cavity loss per turn). This value becomes large as a decreasing number of layers of the cavity mirror, while the cavity loss increases with a decreasing number of layers. Taking into account the estimated FEL gain shown in Fig. 1, we chose multi-layers of 13 and 19 layers for the rear and the front mirror, respectively. With these mirrors, the estimated round-trip cavity loss was 1.4% which is enough small comparing the FEL gain of 1.7 % at a beam current of 50 mA/bunch (one half of maximum beam current stored) and the transmittance of the rear mirror is estimated to 0.4% leading to a cavity efficiency of about 30%. This value is enough large for high power lasing.

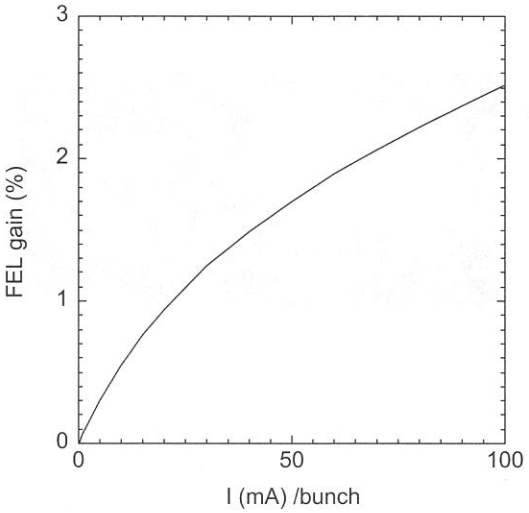

Fig.1 Calculated FEL gain at a wavelength of 240 nm as a function of a beam current taking into account of bunch lengthening due to the potential-well distortion.

Prior to a lasing experiment, we measured round-trip loss of mirrors fabricated by a private company under our instruction discussed previously. The loss measured with the cavity ring down method [3] was about 1.9 % at a wavelength of 240 nm. The value was much larger than the value we expected and this is probably because reflection index at the wavelength was smaller than one we have used for the estimation. Therefore a lasing experiment was made with a beam current of more than 60 mA/bunch to satisfy the threshold condition, i.e.; gain > loss. Since the gain was not well above the loss, an optimization of the optical cavity conditions to obtain the

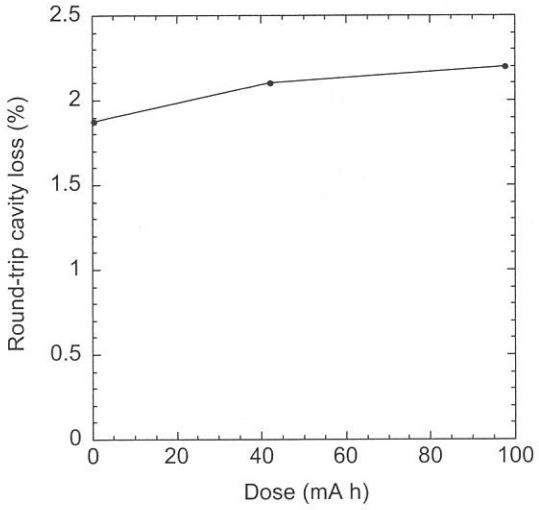

Fig. 2 Measured round-trip cavity loss at a wavelength of 240 nm as a function of dose of exposure to the undulator radiation.

maximum overlap between the electron beam and the laser was very important. If a FEL gain is enough high comparing cavity loss, lasing is possible without perfect overlap between electron and the optimization is possible looking at extracted laser power after the lasing. However, since the lasing was not yet obtained, we had to tune a lot of parameters of the optical cavity without clear target. Furthermore the loss had reached up to 2.2 % as irradiated by the synchrotron radiation during the experiment (Fig.2) and then we had to store the electron beam of more than 75 mA/bunch to satisfy the threshold condition. At this high current, the electron beam decayed very quickly and consequently we have found that the optimization of the optical cavity is impossible.

In conclusion, an experiment on high power UV lasing using a high efficiency mirror was performed but the lasing was not achieved because of the high cavity loss. We have found that much higher FEL gain is necessary for a high power lasing using high efficiency mirrors. This will be satisfied in the upgraded storage ring "UVSOR-II" with an improved gain by at least factor 2.

References

[1] H. Nishno, et. al., J. Am. Chem. Cos. 124 (2002).

[2] H. Hama, et. al., Proc. of the 3rd Asian Symposium on Free Electron Lasers.

[3] P. Elleaum, et. al., Appl. Opt. 24 (1985).

Feasibility Study of Generation of Far Infrared Coherent Synchrotron Radiation Using Ultrashort Laser Pulses at UVSOR

Y.Takashima, M.Katoh[A], M.Hosaka[A] and A.Mochihashi[A]

Department of Materials Processing Engineering, Graduate School of Engineering, Nagoya University, Chikusa-ku Nagoya 464-8603 Japan
[A] UVSOR Facility, Institute for Molecular Science, Okazaki 444-8585 Japan

1. Introduction

We have been considering a method for the generation of far infrared coherent synchrotron radiation from UVSOR storage ring.

Low energy synchrotron radiation is emitted coherently by electrons within a bunch if the wavelength of the radiation is equal and longer than the length of the bunch [1]. The intensity of the coherent radiation is proportional to the square of the number of electrons in a bunch. However, coherent radiations are generally not emitted from a storage ring because the radiations are dumped in the beam pipes if their wavelengths are longer than the dimensions of the beam pipes [1].

Far infrared coherent radiations, which wavelengths are much shorter than the dimension of the beam pipes, can be emitted when the electron bunches have periodic density modulations [2]. In order to obtain intense far infrared synchrotron radiations, we have been studying the feasibility to generate coherent radiations by using the bunch slicing technique [3,4,5,6].

The bunch slice can be achieved by using a laser pulse passing together with an electron bunch through in an undulator [6]. We tune the undulator to the wavelength of the laser, so that the energy of electrons overlapped with the laser are modulated by the interaction with the laser field. If the energy modulation is several times lager than the r.m.s. energy spread of the electron beam, the modulated electrons are separated spatially and a dip is made in the bunch when the electrons pass through a dispersive section as shown in Fig. 1. The modulated electron bunch with a dip can emit coherent radiations, the wavelengths of which is in the same order of the size of the dip.

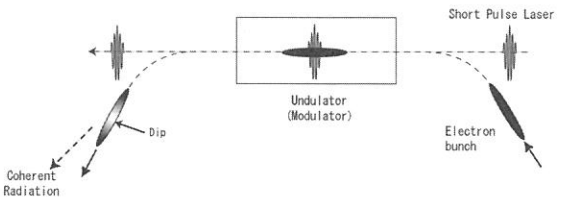

Fig1. Sketch of bunch slicing technique.

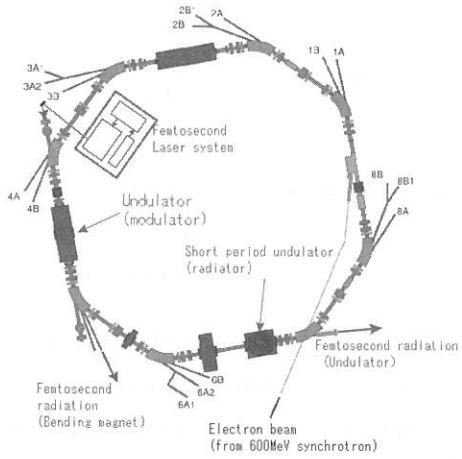

Fig. 2. Layout of experimental equipment.

2. Experimental Equipment

Fig. 2 shows an example of experimental setup to slice the electron bunches. We will use the existing BL5A undulator as an energy modulator in which circulating electrons interact with the laser pulses.

A mode-locked Ti-sapphire laser and an ultrafasst regenerative amplifier is used to make femtosecond laser pulses which should have enough power to make sufficient energy modulation in order to make a dip [6].

3. Intensity of Coherent Radiation

The intensity of the coherent radiation is expressed by the following equations [1,2],

$$\frac{dI}{d\omega}_{multiparticle} = (N + N(N-1)f(\omega))\frac{dI}{d\omega}_{oneparticle}$$

$$= P(\omega)_{incoherent} + P(\omega)_{coherent}$$

$$f(\omega) = \left| \int_{-\infty}^{\infty} e^{\frac{i\omega z}{c}} S(z)dz \right|^2$$

, where I is the intensity of the radiation, ω is the frequency, N is the number of electrons within a bunch, $f(\omega)$ is the Fourier transform of the normalized spatial distribution of electron density of a bunch, $S(z)$, along with the beam direction. $P(\omega)_{incoherent}$ and $P(\omega)_{coherent}$ are the power of incoherent and coherent

radiations, respectively, emitted from a electron bunch. The ratio of the coherent to incoherent radiation intensity is [2],

$$\frac{P(\omega)_{coherent}}{P(\omega)_{incoherent}} \cong N \cdot f(\omega)$$

, because of the large number of N ($\sim 10^{10}$), coherent radiations can dominate over the incoherent radiations.

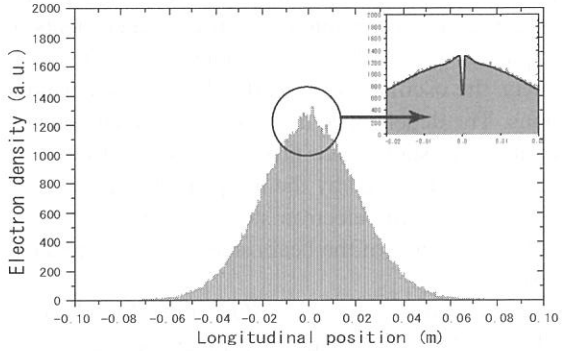

Fig. 3. Electron density distribution at the exit of BM6 with a dip calculated by using SAD code.

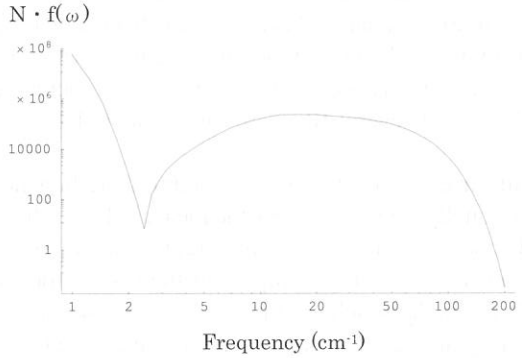

Fig.4. Ratio of the coherent to incoherent radiation intensity, $N \cdot f(\omega)$, at the exit of BM6. N is 2×10^{10} (18mA/bunch).

As shown in Fig.3, the beam tracking simulations has confirmed that a dip can be made in the bunch at the exit of BM6. The SAD code developed in KEK for accelerator design [7] was used for the simulations. The electrons of the width of 1 ps in a bunch were modulated their energy up to 0.8 % in the existing BL5A undulator (modulator) and then traveled to the BM6.

Fig.4 shows the ratio of the coherent to incoherent radiation intensity. For example, at the frequency of 20 cm^{-1} (wavelength is 0.5 mm), the ratio is abut 2×10^5 when the beam current is 18mA/bunch($N$is 2×10^{10}).

In order to improve the intensity of the radiation, we have been considering making dips periodically in one bunch shown as Fig.5. Fig.6 shows the the ratio of the coherent to incoherent radiation intensity for *S(z)* of Fig.5 with the beam current of 18mA/bunch. At the frequency of 12.6 cm^{-1}(wavelength is 0.8mm), $N \cdot f(\omega)$ is 1.6×10^7. The peak intensity is proportional to the square of the number of dips. The peak frequencies are at $2\pi m/l$, m is an integer and l is the distance between dips.

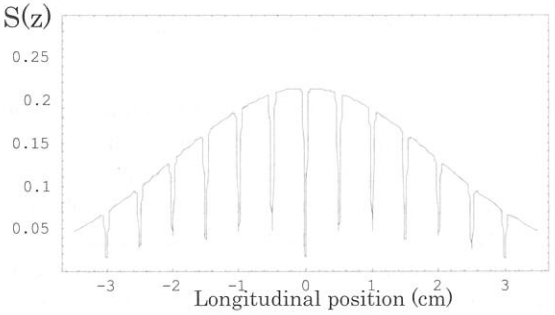

Fig. 5. An example of normalized electron density distribution with 13 periodical dips.

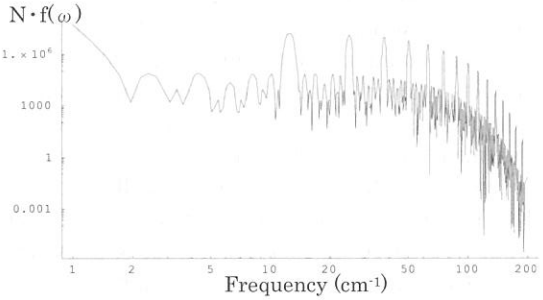

Fig.6. Ratio of the coherent to incoherent radiation intensity, $N \cdot f(\omega)$, for *S(z)* of Fig.5. N is 2×10^{10} (18mA/bunch).

4. Summary

We have been planning to generate far infrared coherent synchrotron radiation using the bunch slicing technique at UVSOR. A commercial short pulse laser can be used to slice electron bunches and make dips which are indispensable to generate the coherent radiations. The averaged intensity of the far infrared coherent radiation is about ten times larger than the incoherent radiation if we use the laser of 5 kHz repetition rate and make one dip in each bunch.

For further studying, we should consider methods to improve the intensity of the radiation, for example, how to make dips periodically in a bunch.

References

[1] H.Weidemann, "Particle Accelerator Physics", Springer-Verlag, (1993)

[2] G.L.Carr et al., Nucl. Instr. and Meth. A463, 387 (2001)

[3] A.A.Zholents and M.S.Zolotorev, Phys. Rev.Lett., 76, 912 (1996)

[4] K.J.Kim, J.Synchrotron Rad., 5, 202 (1998)

[5] R.W.Schoenlein et al., SCIENCE, 287, 2237 (2000)

[6] Y.Takashima et al., UVSOR Activity Report, (2001)

[7] KEK Accelerator Theory Group, http://acc-physics.kek.jp/SAD/sad.html

Ion Trapping Phenomenon in UVSOR[1]

A. Mochihashi, K. Hayashi, M. Hosaka, M. Katoh, J. Yamazaki, Y. Takashima*, Y. Hori**

UVSOR Facility, Institute for Molecular Science, Myodaiji, Okazaki 444-8585, Japan
**Institute for Molecular Science, Myodaiji, Okazaki 444-8585, Japan*
***High Energy Accelerator Research Organization (KEK), Tsukuba 305-0801, Japan*

In the UVSOR, a coherent oscillation of electron bunches in vertical direction has been observed in a multibunch operation, in which a series of bunches (a bunch train) followed by a series of empty buckets (a bunch gap) is stored in the ring[1, 2]. The oscillation amplitude is small enough to neglect influence on users experiments of the synchrotron radiation, however, it can be observed by pickup electrodes with a spectrum analyzer. The oscillation depends on the condition of the vacuum in the ring; namely, the oscillation is clearly observed under poor vacuum conditions and becomes weak in good vacuum conditions. The dependence implies that the phenomenon is caused by ion-trapping[3, 4]. When the ions are trapped, their electrostatic force produces a shift of betatron oscillation frequency (betatron tune) of the electron beam. The tune shift caused by the trapped ions occurs both in the horizontal and in the vertical directions. For flat beams such as in the electron storage ring, the ratio of the vertical tune shift to the horizontal tune shift is approximately the inverse of the beam size, so that in general, vertical tune shift is more prominent than horizontal tune shift[4].

We observed dependence of the vertical tune on the vacuum conditions in the UVSOR-ring. We changed the vacuum conditions by turning off distributed ion pumps (DIPs), that are settled along inner arc wall of the beam ducts at every bending magnet section, and sputtering ion pumps (IPs), that are settled below the beam ducts at every straight section, and measured the vertical tune. In a series of the experiments, we performed the measurement with a multibunch condition in which a series of 12 bunches followed by 4 empty buckets are stored in the ring. This filling pattern is normally adopted for users runs. To measure the vertical tune, we used the RF-KO method with a band-limited noise source (colored noise source) and analyzed beam signals from a pick-up electrode by a spectrum analyzer (Rhode & Schwartz, FSEB30). Figure 1 shows that the tunes changed when the averaged vacuum pressure was intentionally changed. From Fig. 1, it is clearly seen that the vertical tune increases with increase in the vacuum pressure, especially when all the DIPs and several IPs were turned off (14 IPs are settled in the ring, and 4 IPs were switched off in the experiment).

Next, we observed dependence of the vertical tune on the beam current in the multibunch condition (12 bunches + 4 empty buckets) without changing the vacuum conditions intentionally. Figure 2 shows the measured tune shifts from the tunes of the highest beam current in each experiment. Circles and triangles in Fig. 2 represent the results in the multibunch condition but in different vacuum condition. Diamonds in Fig. 2 represent the results for the horizontal tune in Exp. 2. For comparison measured tune shift in single bunch operation is also shown in the figure. Figure 3 shows the change in the averaged pressure in the ring during each experiment. The pressure in the Exp. 2 of the 12-bunch train was higher than in the Exp. 1; this is because we installed a new vacuum chamber in a beamline between these two experiments. As seen in Fig. 2 and 3 the dependence of the tune on the beam current tends to become larger when the vacuum pressure is higher, as seen in the Exp. 1 and 2 in Fig. 2 and 3. On the other hand, the dependence in the singlebunch condition was much smaller than in the multibunch conditions although the bunch current in the singlebunch and the multibunch conditions were the same. The fact that the change in the horizontal tune in Exp. 2 is very small compared to that in the vertical tune also indicates that the change in the vertical tune in the multibunch condition is caused by the ion-related phenomenon.

Vertical tune shift $\Delta\nu_y$ due to the trapped ions is written as[4]

$$\Delta\nu_y = \frac{r_e E_0}{2\pi E}\lambda_e \eta \int_C \frac{\beta_y(s)}{\sigma_y(s)\left(\sigma_x(s)+\sigma_y(s)\right)} ds, \tag{1}$$

where r_e the classical electron radius, E_0 the rest mass of the electron, E the total energy of the electron, λ_e the averaged line density of the electrons, η the neutralization factor, $\beta_y(s)$ the vertical betatron function and $\sigma_{x,y}(s)$ the horizontal/vertical beam size, respectively. In Eq. (1) the tune shift is proportional to the line density of the electron λ_e; namely, the tune decreases as the beam current decreases. For the Exp. 1 and 2 in Fig. 2, however, the vertical tune increases with decrease in the beam current just contrary to the prospect from Eq. (1). One of causes of the disagreement is that the neutralization factor η might strongly depend on the beam current; namely, in Fig. 2 the neutralization factor could increase largely as the beam current decreases.

We have estimated theoretically the dependence of the neutralization factor on the beam current by evaluating a capture rate of the ions as a ratio of the number of the trapped ions to total number of the created ions. According

[1] submitted to Physical Review Special Topics - Accelerators and Beams

to the theoretical model[5], the neutralization factor η is written as

$$\eta = \frac{D_0}{D_e}\alpha, \tag{2}$$

where D_0 is the residual gas density, $D_e$is the electron density in the beam and α is the capture rate of the ions, respectively. From Eq. (2) we have calculated the rate with both an analytic method that is from the classical theory of the ion trapping[3, 4] and a tracking method that tracks motion of the ions under continuous passage of the electron bunch train. Figure 4 (a) shows the change in the capture rates (α) on the beam current from both the analytic and the tracking calculations. In the calculation, we only consider CO that is the main component of the residual gas in the UVSOR-ring. As the trapped ions, we only consider CO^+ ions that are created in scattering between the CO and the circulating electrons[6]. The α in Fig. 4 (a) corresponds to the value that is averaged over the ring circumference. It is clearly seen that the capture rates increase as the beam current decreases. To estimate the neutralization factor (η) from Eq. (2), it is necessary to consider not only the dependence of the α on the beam current but also the dependence of the residual gas density (D_0) on the beam current. Moreover, for the estimation of the η it is necessary to evaluate the D_0 on the beam orbit, that is difficult to measure directly. Here, we have used the averaged pressure (Fig. 3) measured by the vacuum gauges which are located near the ion pumps to evaluate the D_0. Even though the vacuum pressure at the vacuum gauges is not necessarily the same as that on the beam orbit, it must reflect the change in the D_0 on the beam current. The averaged pressures during each experiment (Exp. 1 and 2) in Fig. 3 are plotted again in Fig 4 (a). From the theoretical value of the capture rates and the measured value of the averaged vacuum pressure with the vacuum gauges, we have estimated the neutralization factor during each experiment with Eq. (2). Figure 4 (b) shows the neutralization factors during the experiments in the multibunch condition. The curves and marks correspond to the η estimated with the α from the analytic and tracking calculations, respectively. As seen in the figure, the neutralization factor largely increases despite the decrease in the beam current, especially in 15$\sim$30 mA/bunch.

With the neutralization factors in Fig. 4 (b) and Eq. (1), we have estimated the dependence of the vertical tunes on the beam current for the multibunch condition. The analytic and tracking results for the experiments in the multibunch condition are shown in Fig. 5 with each experimental results. As seen in the figure, the results of the tracking calculations agree qualitatively with the experiments, though the averaged pressures measured by the vacuum gauges are used to evaluate the neutralization factors, as discussed above. As a measure, we analyzed change in the vertical tune with the bunch current $\left(\frac{\Delta\nu_y}{\Delta I_b}\right)$ for the region in which the bunch current is higher than 15 mA. For $\left(\frac{\Delta\nu_y}{\Delta I_b}\right)$ in Exp. 1, $-1.16\times10^{-4}\pm2.4\times10^{-6}$/mA is obtained in the experiments and -1.77×10^{-4}/mA is obtained from the tracking. For Exp. 2, $-2.02\times10^{-4}\pm5.0\times10^{-6}$/mA in the experiment and -2.28×10^{-4}/mA from the tracking are obtained, respectively. The tracking results reproduce the experiments performed in different conditions of the vacuum. In the region where the bunch current is lower than 15 mA, the agreement between the tracking results and the experiments are not as good as in the higher bunch current; the tracking results tend to underestimate the change in the vertical tune. The disagreement might be explained by the contribution of other ion species on the neutralization factor; namely, the contribution of the effect of the dissociated O^+ and C^+ ions. Another cause of the disagreement between the tracking calculations and the experimental results is that we have used the averaged vacuum pressure measured by the vacuum gauges to evaluate the residual gas density (D_0): the vacuum pressure on the beam orbit is not necessarily the same as that at the vacuum gauges. Moreover, in general, the vacuum pressure depends on the position along the ring circumference. Because the capture rate depends not only on the beam current but also the position along the ring circumference it is complicated to estimate the η exactly. The tracking results, however, reproduce not only the tune shift that depends on the beam current but also the difference of the dependence of the tune shift on the vacuum pressure. As seen in Fig. 5, the results from the analytic calculations qualitatively agree with the experiments, though the results overestimate the change in the vertical tune compared to both the experimental results and tracking calculations. This is because in the analytic calculation[5] the stability condition can be only considered; all the CO^+ ions are trapped and never go away from the beam. Therefore, the analytic calculation tends to overestimate the neutralization factor.

References

[1] A. Mochihashi, in *Proceedings of 8th European Particle Accelerator Conference, Paris, 2002*, edited by T. Garvey, p. 1939.

[2] A. Mochihashi *et al.*, UVSOR Activity Report 2001, p. 41.

[3] R. D. Kohaupt, DESY Interner Bericht No. H1-71/2, 1971 (unpublished).

[4] Y. Baconnier, G. Brianti, CERN Internal Report No. CERN/SPS/80-2 (DI), 1980 (unpublished).

[5] A. Mochihashi *et al.*, Physical Review Special Topics - Accelerators and Beams [submitted].

[6] P. A. Redhead, Can. J. Phys. **47**, 2449 (1969).

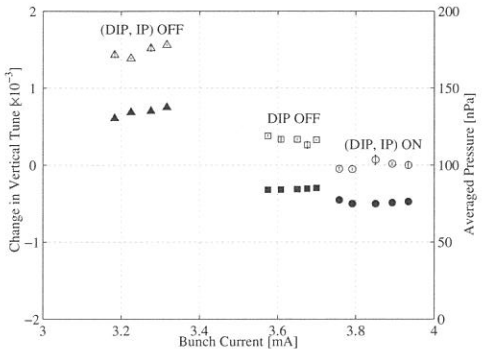

Figure 1: The change in the vertical tune and the averaged pressure when the ion pumps were intentionally turned off. Empty and filled marks correspond to the change in the vertical tune and the averaged pressure, respectively. The marks correspond to the change in the tune and the averaged pressure when all the DIPs and IPs were turned on (circles), all the DIPs were turned off (squares) and all the DIPs and several IPs were turned off (triangles), respectively.

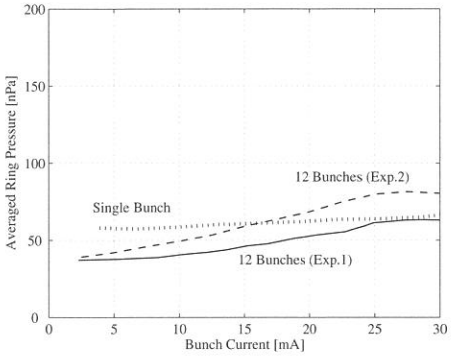

Figure 3: The averaged vacuum pressure for each experiment in Fig. 2.

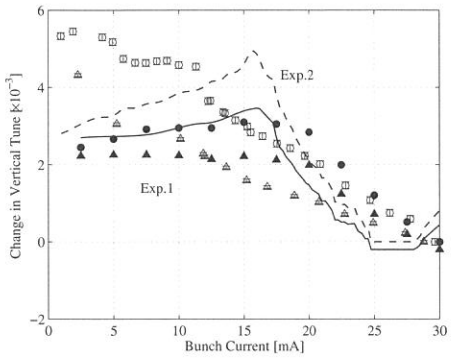

Figure 5: The experimental results, tracking calculation and the analytic calculations of the change in the vertical tunes in the 12-bunch train. Empty triangles, filled triangles and solid curve correspond to the experiments, the tracking and the analytic results for Exp. 1, respectively. Empty/filled circles and a broken curve are for Exp. 2.

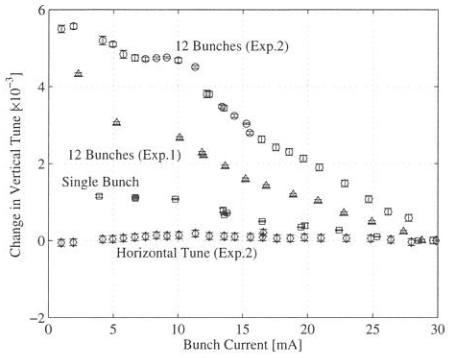

Figure 2: Dependence of the vertical tune on the beam current in the multibunch condition but in different vacuum condition (Exp.1 and 2), and in the single-bunch condition.

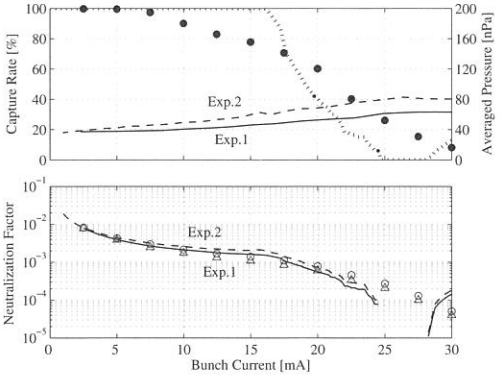

Figure 4: (a) The analytic (dotted curve) and tracking calculations (filled circles) of the capture rates. The averaged vacuum pressure (see Fig. 3) for the experiments (Exp. 1 and 2) in the multibunch condition measured by the vacuum gauges are also plotted (solid and broken curves). (b) The neutralization factors (η) evaluated from the theoretical value of the capture rates and the measured value of the averaged vacuum pressures for the experiments. Triangles and solid curve correspond to the η estimated with the capture rates from the analytic and tracking calculations in Exp. 1, respectively. Circles and a broken curve are for Exp. 2.